

EFFECTS OF ELEVATED TEMPERATURE AND RE-CURING ON THE PROPERTIES OF MORTARS CONTAINING INDUSTRIAL WASTE MATERIALS*

N. U. KOCKAL

Dept. of Civil Engineering, Akdeniz University, 07058, Antalya, Turkey
Email: nukockal@akdeniz.edu.tr

Abstract– Behavior of mortars with and without silica fume (SF), containing green ceramic powder (GCP) and marble dust (MD) under the conditions of pre-fire and post-fire was investigated. In addition, influence of re-curing on the mechanical properties and permeability of fire-damaged high-strength mortars was studied. For this purpose, mortars subjected to 800 °C were water-cured for 7 days after air-cooling. In order to determine the physical, mechanical and permeability properties of mortars, the bulk density, water absorption, porosity, flexural and compressive strength, capillary water absorption tests were conducted and optical microscope analyses were also performed. Results showed that mortars with MD had the highest strength values and the lowest permeability for normal and post-fire conditions, however, mortars with GCP showed the best performance among other mortars after re-curing. This can be attributed to the siliceous composition of GCP regarding the vulnerability at high temperature and suitability in C-S-H re-formation when re-curing. Water-curing contributed to re-hydration and self healing, resulting in strength re-gain and porosity recovery which was also observed by microstructural evaluation.

Keywords– Mortar, marble dust, green ceramic powder, fire, re-curing, recovery

1. INTRODUCTION

The strength and durability of concrete decrease at elevated temperatures due to chemical and physical changes although concrete is noncombustible and generally provides adequate fire resistance for most normal applications [1, 2]. Cement-based materials may be subjected to high temperatures in normal service conditions, such as in nuclear power plants, radioactive waste storage facilities, or under accidental conditions, for instance, during fire incidents in buildings and tunnels. Temperature variations and heating/cooling cycles may also be encountered [3]. Different approaches can be taken in order to protect a building structure depending on the risk level, the required resistance time and materials involved [4]. Some investigations were performed to determine the effects of high temperatures on concrete and mortar properties [5-9]. Some researchers also studied the relationship between surface color changes and different elevated temperatures [10-13], others conducted various techniques such as the drilling resistance test [14], hot guarded plate test [15] and micro-mechanical analysis [3] in order to assess the residual capacity of fire-damaged concretes and mortars.

In recent years, industrial waste materials have been widely used in the construction field due to the increasing need to recycle these materials in order to protect the environment. However, very few research works have been published on the use of GCP and MD in concrete and mortar mixtures. Unfortunately, they are often associated with shortcomings such as the need to determine the behavior of mortars before

*Received by the editors November 24, 2011; Accepted March 1, 2012.

and after exposure to elevated temperature. Also, the effect of utilizing both GCP and MD on mortar properties is not well documented in the literature. Therefore, this study investigated the potential benefits of using GCP and MD in mortars under the conditions of pre-fire, post-fire and re-curing by evaluating their effects on the strength and the permeability characteristics of mortars.

2. MATERIALS AND METHODS

a) Materials used in mortar production

The chemical compositions of materials used in mortar mixes are exhibited in Table 1. The cement used was ordinary Portland cement CEM I 42.5R according to the European Standards EN 197-1 [16]. The Blaine fineness of cement was 319.4 m²/kg and its relative density (specific gravity) was 3.13. Calcareous natural sand which originated from Dirmil, Burdur located in the southwest of Turkey was used. Its relative density and water absorption were 2.69 and 2.0%, respectively. Its particle size distribution is shown in Table 2. MD was obtained from a marble company in Antalya as a by-product of marble sawing and shaping in sludge condition. Its relative density was 2.64. SF used had a specific gravity 2.24 and its activity index was 131.50 %. GCP was provided from a local tile company and its specific gravity was 2.63. Chemical admixture used to adjust consistency was a sulphonated polymer-based superplasticizer.

Table 1. Chemical compositions of materials used in mortar preparation by weight (%)

Materials	LOI ^a	Na ₂ O	MgO	Al ₂ O ₃	SiO ₂	ZrO ₂	SO ₃	K ₂ O	CaO	ZnO	Fe ₂ O ₃
Cement	3.39	0.11	1.08	5.41	19.86	-	2.70	0.74	62.24	-	3.60
Silica fume	1.33	0.49	1.25	0.62	91.97	-	0.35	1.49	0.31	-	1.32
Cer. powder	6.80	1.47	1.02	16.81	55.18	3.3	0.18	1.91	7.97	2.29	0.80
Marble dust	44.90	-	0.94	0.41	4.53	-	-	-	51.34	-	0.04

^a Loss on Ignition

Table 2. Particle size distribution of calcareous sand

Sieve size (mm)	8	4	2	1	0.500	0.250	0.125	0.063
Passing (%)	100	97.2	70.4	44.4	27.7	17.8	10.7	5.1

b) Mix design and preparation of mortars

Nine different types of mortar mixes were prepared and their mix proportions and notations are given in Table 3. The w/c ratio was 0.50 and the sand:binder ratio was 3:1. Cement was replaced with SF in varying proportions (5% and 10%). Sand was replaced with MD and GCP in a ratio of 16 % and 4 % of grains passing through 0.250 mm and 0.063 mm sieves, respectively. All substitutions were made in weight. Because of the different physico-chemical characteristics of both by-products, different superplasticizer ratios were needed for each formulation. Replacement of GCP with sand, even in small amounts, made the mixture consistency more muddy causing difficulties during compaction owing to the clay mineral content. Therefore, different replacement percentages of these two materials were determined due to the consistency adjustments. The flow diameter values of fresh mortar mixtures were kept constant as 212±13 mm.

All sample preparations were processed in a similar manner, according to European Standard EN 196-1 [17]. The mortars were cast into 40x40x160 mm prismatic and 100 mm cubic moulds for 24 h. The hardened mortar specimens were then demoulded and maintained under lime-saturated water at 20 ± 2 °C until the age of testing.

Prismatic specimens were subjected to temperature of up to 800 °C at an incremental rate of 13 °C per minute from room temperature, using an electrically-heated furnace designed for a maximum temperature of 1200 °C. The cube specimens were exposed to the same temperature with lower heating rate (6 °C per

minute) due to the risk of disruption by explosion of thick sectioned specimens with waste materials in the furnace. The temperature was sustained at 800 °C for 10 minutes before the specimens were allowed to cool to 600 °C (cooling rate 16 °C/min) inside the furnace. The specimens were then taken out from the furnace to cool in the laboratory conditions for 24 hours. After cooling, half of the specimens were tested and the other half re-cured in water for 7 days. Re-cured mortars were tested to determine the properties re-gained.

Table 3. Mix proportions (g), flow diameters and notations of mortars

Specimen	Sand	Cement	Silica fume	Ceramic powder	Marble dust	Chemical Admixture	Flow diameter (mm)
K0	1350	450	-	-	-	1.3	220
K5	1350	427.5	22.5	-	-	1.5	215
K10	1350	405	45	-	-	3.0	200
S0	1296	450	-	54	-	4.0	225
S5	1296	427.5	22.5	54	-	5.8	201
S10	1296	405	45	54	-	9.0	206
M0	1134	450	-	-	216	5.5	203
M5	1134	427.5	22.5	-	216	7.0	200
M10	1134	405	45	-	216	10.0	204

c) Experimental procedures

Consistency of mortars was measured by the flow table test according to ASTM C 270 [18]. The test procedure involves placing the mould in the center of the flow table and filling it in two layers, each layer being tamped 20 times with the tamper. The table was then jolted 25 times, and the diameter of the spread mortar was measured in two directions at right angles to each other using callipers.

The bulk density, water absorption and porosity values were obtained by testing both 100 mm cube and 40x40x160 mm prism specimens according to ASTM C 642 [19] by using the equations given below:

$$A = W_1 / (W_2 - W_3) \quad (1)$$

$$B = W_1 / (W_1 - W_3) \quad (2)$$

$$C = ((W_2 - W_1) / (W_2 - W_3)) * 100 \quad (3)$$

$$D = ((W_2 - W_1) / W_1) * 100 \quad (4)$$

where, A is the dry bulk density; B is the apparent bulk density; C is the apparent porosity (%); D is the water absorption by weight (%); W_1 is the mass of oven-dried sample in air (g); W_2 is the mass of surface-dry sample in air (g) and W_3 is the mass of surface-dry sample in water (g).

The flexural and compressive strength of hardened mortar specimens were determined in accordance with EN 1015-11 [20]. The flexural strength of a hardened mortar was evaluated by three point loading of a 160x40x40 mm prism specimen, subsequent to the failure and breakage of this specimen the compressive strength was determined on each half of the prism specimen.

Capillary water absorption test was carried out with the 100 mm cube specimens by measuring water contents absorbed at 1, 4, 9, 16, 25, 36, 49, 64 and 1440 minutes. The capillary absorption coefficient was obtained using the following equation:

$$K = Q / (A * t^{1/2}) \quad (5)$$

where, K is the coefficient of capillarity ($\text{cm/s}^{1/2}$); Q is the amount of water absorbed (cm^3); A is the area of the surface exposed to the water (cm^2) and t is the time (s).

Three specimens of each formulation were prepared for each test.

Optical microscope analysis was performed on representative specimens to detect the state of paste matrix, aggregate and transition zone before heating and the cracks formed after heating and re-curing using Nikon Eclipse optical microscope.

3. RESULTS AND DISCUSSION

The bulk density, water absorption and porosity values of 28-day mortar specimens are given in Table 4. With the presence of MD and GCP, dry bulk density values increased while apparent bulk density values decreased in the case of increase in silica fume content. Similarly, ratios of water absorption and apparent porosity decreased with the addition of waste materials. This effect was more pronounced for mixtures with MD, ratios of absorption and porosity reduced to 2.97 % and 6.57 %, respectively, at maximum SF content. This can be attributed to the effective volumetric occupation of waste materials, and thus microfiller effect resulting in densified microstructure of specimens through filling of the finer pores in 28 days [21] and a decrease in porosity of mortars due to the high fineness and low specific gravity, relative to that of cement.

Table 4. Bulk density, absorption and porosity of mortars

Specimen	Dry bulk density	Water absorp. (% wt.)	Apparent bulk density	Apparent porosity (%)
K0	2.09	8.94	2.57	18.68
K5	2.12	6.47	2.46	13.72
K10	2.18	4.79	2.43	10.43
S0	2.18	4.64	2.43	10.11
S5	2.19	4.29	2.41	9.37
S10	2.20	3.55	2.39	7.81
M0	2.19	4.47	2.43	9.78
M5	2.20	3.50	2.38	7.68
M10	2.21	2.97	2.37	6.57

Figures 1 and 2 illustrate the variations in flexural strength values of the 28 and 56-day mortars in the case of pre-fire, post-fire and re-curing after elevated temperature application. Flexural strength values of 28-day specimens with 5% silica fume slightly dropped, whereas specimens with 10 % silica fume relatively increased. However, 56-day specimens showed significant rise in flexural strength with the increase in silica fume. This could be explained by the very fine particles of silica fume with high pozzolanic reactivity [22, 23] and thus, improvement of aggregate-paste interfacial zone in 56 days which is more important for specimens, especially under flexure. In the pre-fire and post-fire conditions, the highest flexural strength values were obtained by the specimens with MD while specimens with GCP showed the most strength regain after re-curing. This indicates that excessive marble dust containing calcium carbonate does not participate in hydration reaction and worked as filler [24]. These strength gain ratios were recorded as 53%; 58%; 60% and 72%; 79%; 80% for S0, S5 and S10, 48%; 50%; 55% and 63%; 65%; 69% for K0, K5 and K10, 41%; 41%; 43% and 45%; 47%; 56%, for M0, M5 ve M10 at 28 and 56 days, respectively.

Compressive strength values of the mortars at 28 and 56 days are exhibited in Figs. 3 and 4. As expected, compressive strength increased with increase in silica fume content at all ages but this rise was remarkably noticeable among 56-day specimens. When making a comparison between specimens without silica fume and specimens with silica fume substitutions of 5 and 10%, these increases were nearly 21%

and 31% for K coded specimens, 18% and 30% for S coded specimens and 21% and 25% for M coded specimens. Similar to flexural strength results, specimens with MD exhibited good performance before and after elevated temperature exposure whereas after re-curing, specimens with GCP had higher compressive strength values. This result may be due to the lack of the siliceous and the aluminous compounds in MD which are necessary for re-hydration. However, ratio of compressive strength loss after elevated temperature application and ratio of compressive strength gain after re-curing were slightly low compared to the ratios of flexural strength. Before elevated temperature exposure, among the 56-day specimens with 10% silica fume, the compressive strength values of specimens containing GCP and MD reached up to 84.0 and 88.4 MPa, respectively. Relative strength loss ratios of control specimens (coded as K) subjected to elevated temperature were larger than specimens with MD and GCP and were between 50 and 56%. Specimens with MD had the lowest strength gain ratios after re-curing which were between 12 and 25% at all ages.

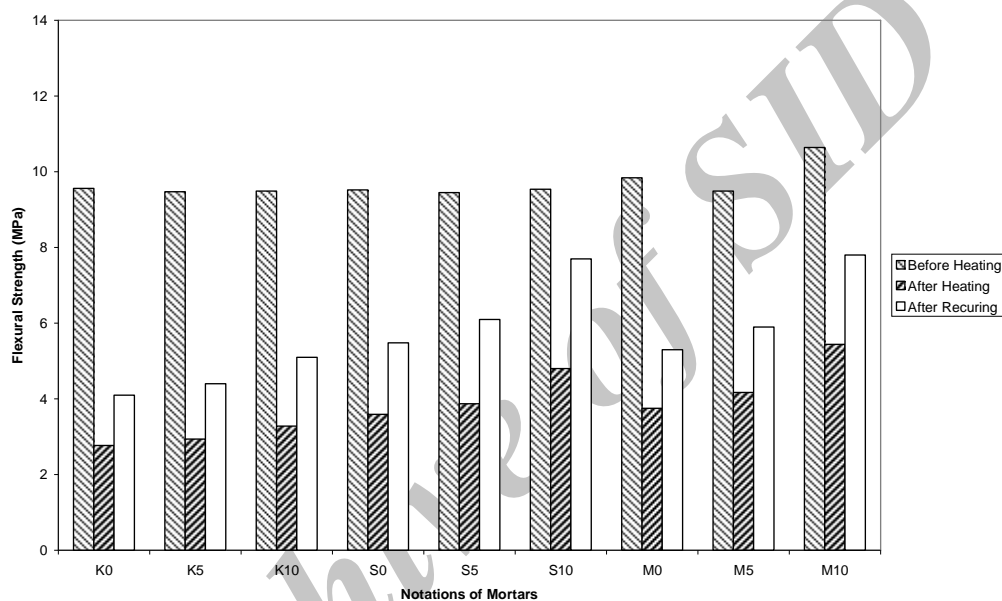


Fig. 1. Flexural strength values of mortars at 28 days

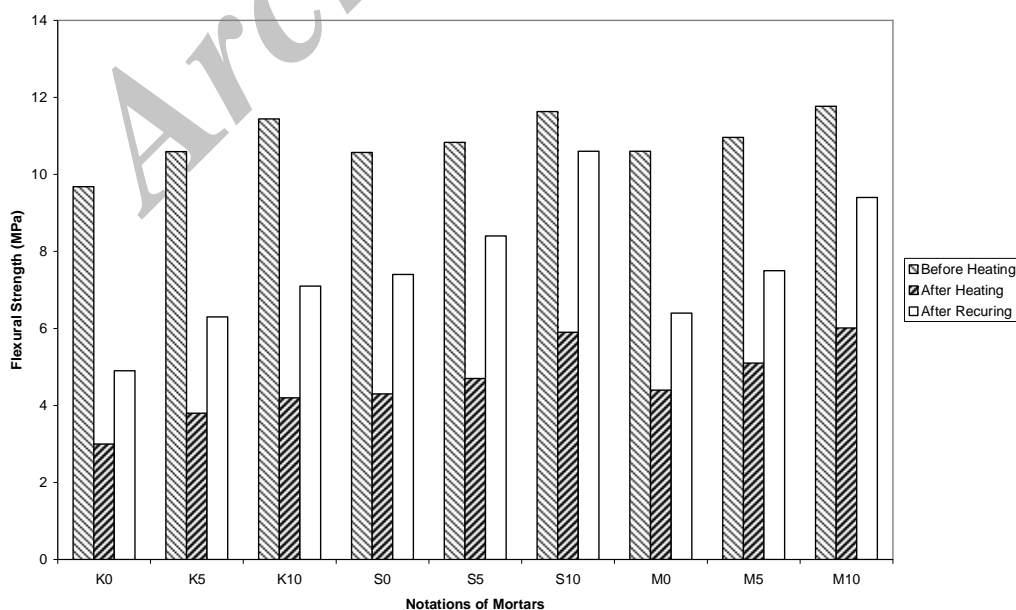


Fig. 2. Flexural strength values of mortars at 56 days

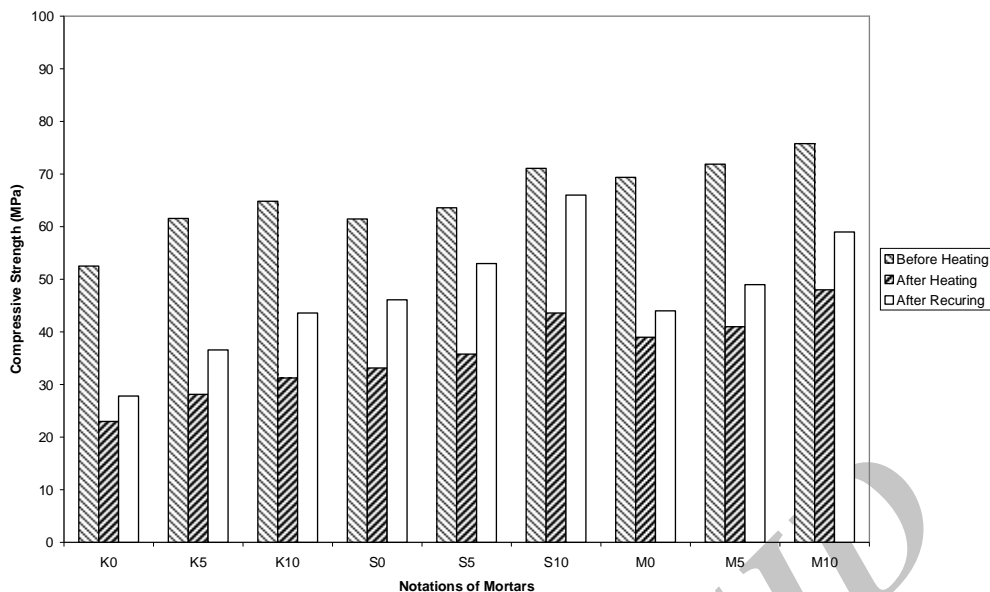


Fig. 3. Compressive strength values of mortars at 28 days

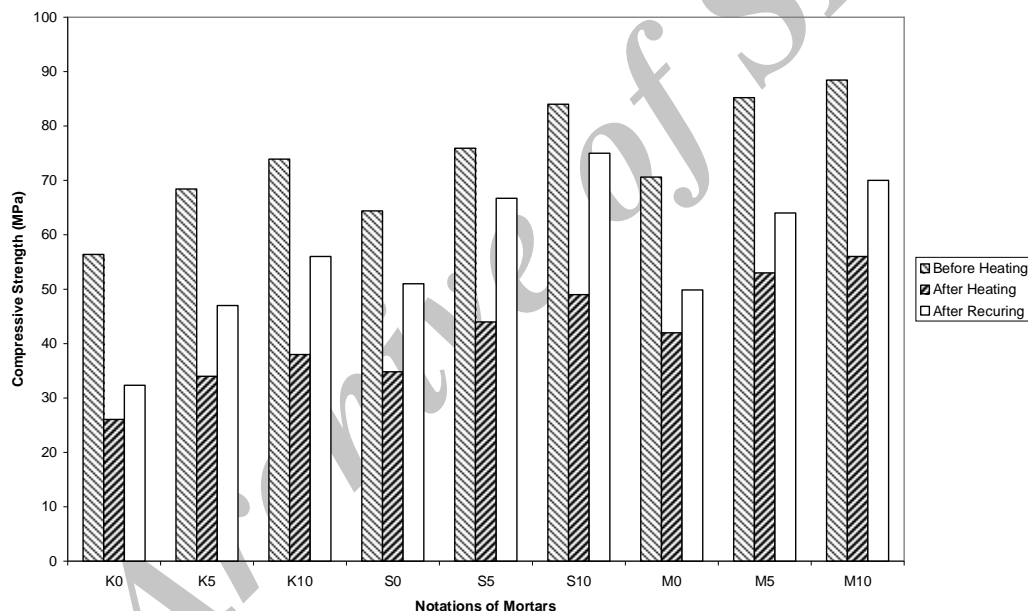


Fig. 4. Compressive strength values of mortars at 56 days

Figures 5 and 6 show the capillarity coefficient of mortars at 28 and 56 days. Sorption is the result of capillary movement in the pores in the concrete which are open to the ambient medium. Among the 28 and 56-day untreated specimens, the highest and lowest values were $17.9 \text{ cm/s}^{1/2}$; $16.2 \text{ cm/s}^{1/2}$ and $4.69 \text{ cm/s}^{1/2}$; $2.8 \text{ cm/s}^{1/2}$ which were achieved by K0 and M10 specimens, respectively. Similarly, after heat treatment, the lowest and the highest coefficients were achieved by the same coded specimens. At the end of re-curing, S coded specimens had the highest recovery while M coded specimens had the lowest. This result may be attributed to higher pozzolanic activity of GCP, generating large number of nucleation sites for the precipitation of the hydration products and thus accelerating cement hydration [25]. The gain ratios at 28 and 56 days were approximately 57%; 63%; 65% and 63%; 69%; 70% for K coded specimens, 63%; 66%; 70% and 64%; 69%; 72% for S coded specimens, 43%; 45%; 48% and 39%; 47%; 49% for M coded specimens, respectively.

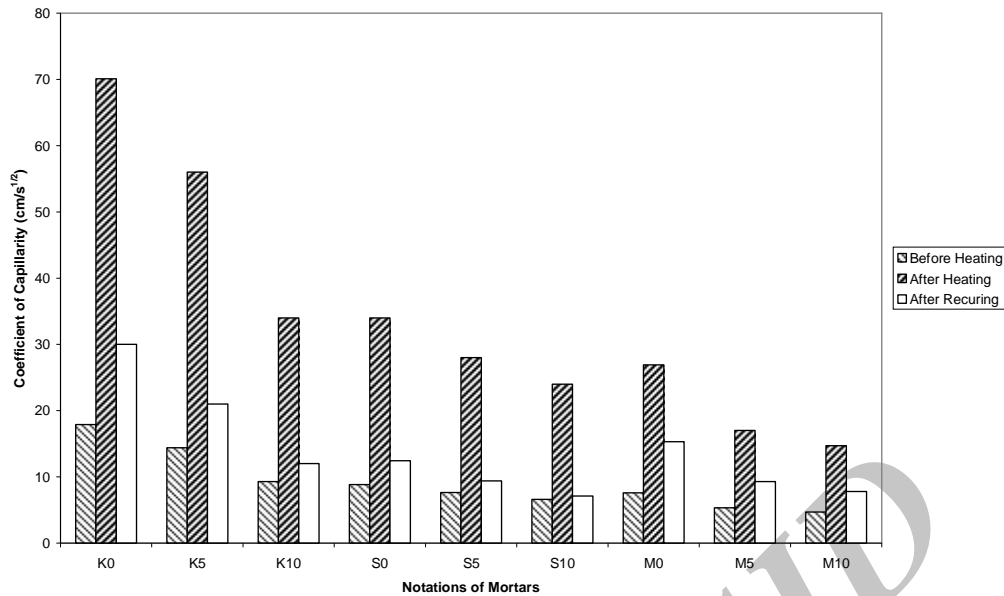


Fig. 5. Coefficient of capillary absorption values of mortars at 28 days

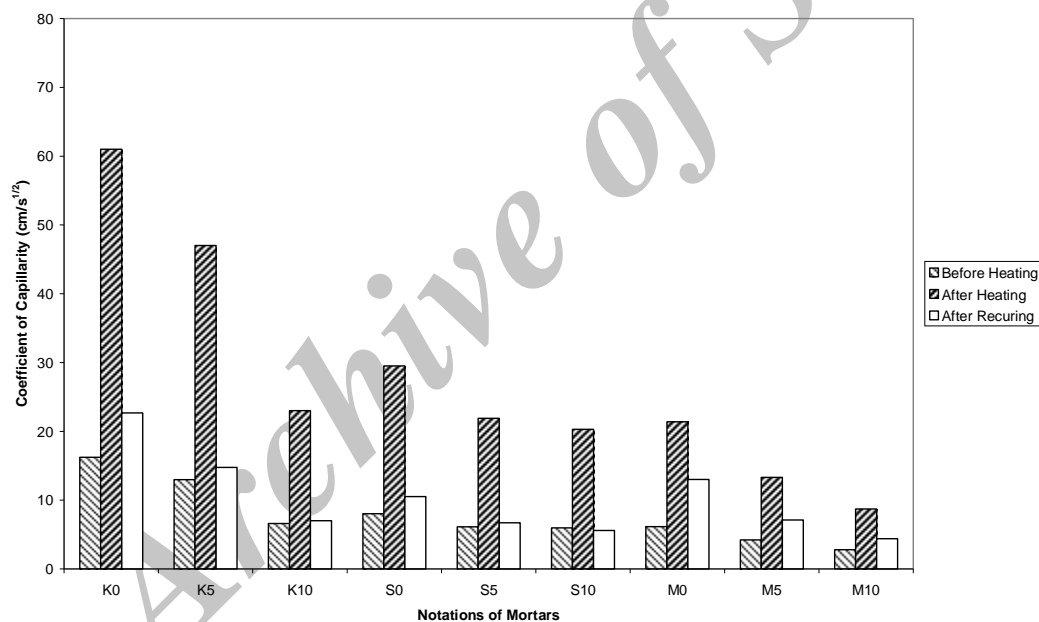


Fig. 6. Coefficient of capillary absorption values of mortars at 56 days

The optical microscope images are exhibited in Figs. 7-9. Microstructure of untreated mortars was analyzed in Fig. 7. It is observed that aggregate particles were uniformly distributed and diameters of pores reached up to 100 microns in the matrix. Mortars with silica fume formed a very dense structure of the hydrated products through both filler and pozzolanic effects, also observed by other researchers [26, 27]. On the other hand, although the destruction was generally in the aggregate- cement matrix interfacial zone of the mortar specimens exposed to elevated temperature, a small number of cracks was propagated through the aggregate particles (Fig. 8). This type of propagation was more pronounced in control specimens. According to the images in Fig. 9, it can be seen that re-curing decreased the thickness of cracks, both in the cement paste and in the transition zone. These results showed parallelism with the strength gain and decrease in porosity for 7- day re-cured specimens. GCP behaved as pozzolanic material due to its clay constituents calcined [28, 29] during heating up to 800 °C. Therefore, owing to re-

hydration, the highest strength recovery took place due to the cement hydration [30] and contribution of sintered GCP to hydration.

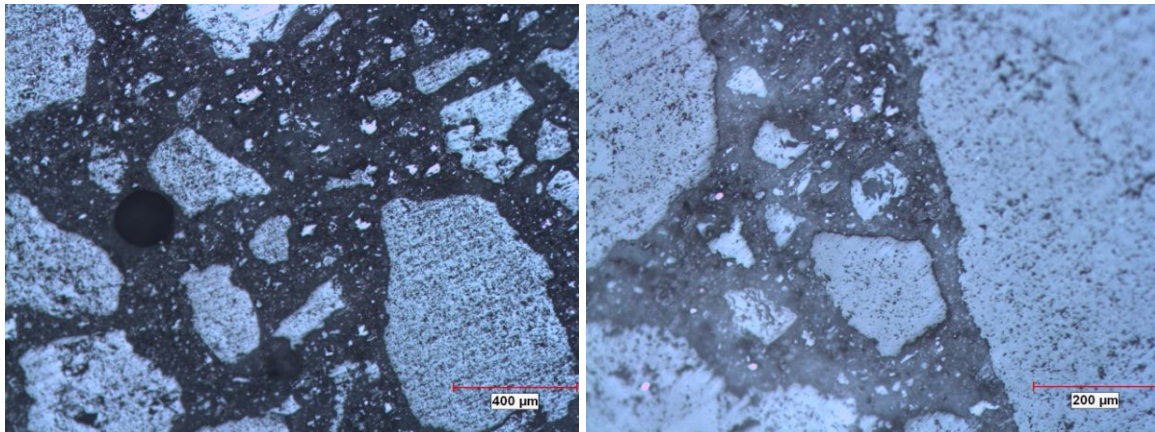


Fig. 7. Common view of mortar specimen before exposure to elevated temperature at 28 and 56 days and at two magnification levels

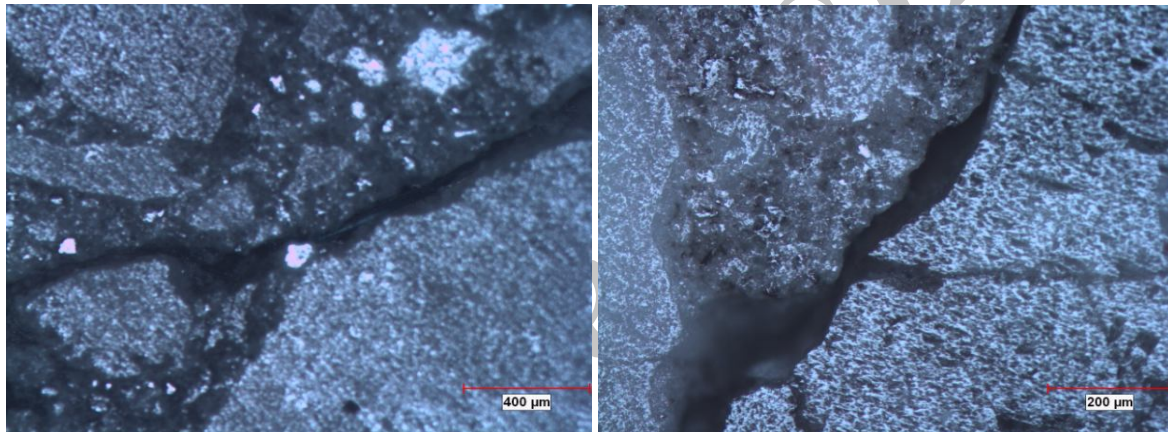


Fig. 8. Common view of mortar specimen after exposure to elevated temperature at 28 and 56 days and at two magnification levels

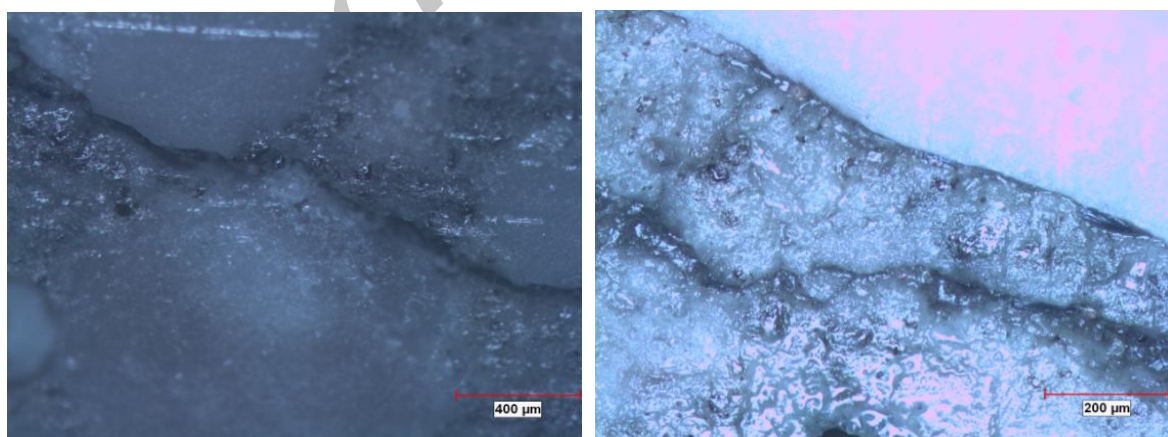


Fig. 9. Common view of mortar specimen after re-curing at 28 and 56 days and at two magnification levels

4. CONCLUSION

From the investigation results presented above, the following conclusions were made:

Mortars with silica fume had a better resistance to elevated temperature than those without silica fume, as also reported previously by many researchers. In addition, the best performances were obtained by mortars containing MD in the case of pre-heat and post-heat treatments and by mortars containing GCP in the case of re-curing. Although mortars containing GCP exhibited low resistance to elevated temperature compared to mortars containing MD having high calcium carbonate content, the siliceous and the aluminous compositions of GCP contributed to additional C-S-H formation when recured in water. This occurrence was also detected in optical microscope analysis by observing improvement of cracks.

Besides, the explosion of 100 mm cubic specimens at temperature between 600 and 700 °C during heating suggested that using these waste materials in thick-sectioned mortar and/or concrete elements may be detrimental where the temperature increase is high. This explosion may be attributed to the absence of porosity in high strength mortars which entrapped gas released from the phase variations of GCP and high loss on ignition of MD. The entrapped gas could not find enough space to decrease stress accumulation at this temperature range. Therefore, it is recommended that further investigations be carried out to make improvements in order to provide a more efficient use of these materials in mortar and concrete, including considerations for exposure to elevated temperatures.

REFERENCES

1. Shoaib, M. M., Ahmed, S. A. & Balaha, M. M. (2001). Effect of fire and cooling mode on the properties of slag mortars. *Cement and Concrete Research*, Vol. 31, pp. 1533–1538.
2. Kong, D. L. Y. & Sanjayan, J. G. (2010). Effect of elevated temperatures on geopolymer paste, mortar and concrete. *Cement and Concrete Research*, Vol. 40, pp. 334–339.
3. Chen, X. T., Davy, C. A., Shao, J. F. & Skoczylas, F. (2010). Experimental and micro-mechanical analysis of the mechanical and transport properties of mortar containing heat-induced micro-cracks. *Cement and Concrete Composites*, Vol. 32, pp. 678–685.
4. Formosa, J., Chimenos, J. M., Lacasta, M., Haurie, L. & Rosell, J. R. (2011). Novel fire-protecting mortars formulated with magnesium by-products. *Cement and Concrete Research*, Vol. 41, pp. 191–196.
5. Sancak, E., Sari, Y. D. & Simsek, O. (2008). Effects of elevated temperature on compressive strength and weight loss of the light-weight concrete with silica fume and superplasticizer. *Cement and Concrete Composites*, Vol. 30, pp. 715–721.
6. Lion, M., Skoczylas, F., Lafhaj, Z. & Sersar, M. (2005). Experimental study on a mortar. Temperature effects on porosity and permeability. Residual properties or direct measurements under temperature. *Cement and Concrete Research*, Vol. 35, pp. 1937–1942.
7. Liu, C. T. & Huang, J. S. (2009). Fire performance of highly flowable reactive powder concrete. *Construction and Building Materials*, Vol. 23, pp. 2072–2079.
8. Peng, G. F., Bian, S. H., Guo, Z. Q., Zhao, J., Peng, X. L. & Jiang, Y. C. (2008). Effect of thermal shock due to rapid cooling on residual mechanical properties of fiber concrete exposed to high temperatures. *Construction and Building Materials*, Vol. 22, pp. 948–955.
9. Kodur, V. K. R., Bisby, L. A. & Green, M. F. (2006). Experimental evaluation of the fire behaviour of insulated fibre-reinforced-polymer-strengthened reinforced concrete columns. *Fire Safety Journal*, Vol. 41, pp. 547–557.
10. Lin, D. F., Wang, H. Y. & Luo, H. L. (2004). Assessment of fire-damaged mortar using digital image process. *Journal of Materials in Civil Engineering*, Vol. 16, pp. 383–386.
11. Yüzer, N., Aköz, F. & Öztürk, L. D. (2004). Compressive strength–color change relation in mortars at high temperature. *Cement and Concrete Research*, Vol. 34, pp. 1803–1807.
12. Luo, H. L. & Lin, D. F. (2007). Study the surface color of sewage sludge mortar at high temperature. *Construction and Building Materials*, Vol. 21, pp. 90–97.

13. Arioz, O. (2007). Effects of elevated temperatures on properties of concrete. *Fire Safety Journal*, Vol. 42, pp. 516–522.
14. Felicetti, R. (2006). The drilling resistance test for the assessment of fire damaged concrete. *Cement and Concrete Composites*, Vol. 28, pp. 321–329.
15. Othuman, M. A. & Wang, Y. C. (2011). Elevated-temperature thermal properties of lightweight foamed concrete. *Construction and Building Materials*, Vol. 25, pp. 705–716.
16. TS EN 197-1. (2002). Cement—composition, specifications and conformity criteria—part 1: common cements. *TS EN 197-1*, TSE Ankara, (in Turkish).
17. TS EN 196-1. (2002). Methods of testing cement—part:1 determination of strength. *TS EN 196-1*, TSE Ankara, (in Turkish).
18. ASTM C 270. (2010). Standard Specification for Mortar for Unit Masonry. *ASTM C 270*, ASTM Philadelphia.
19. ASTM C 642. (2006). Standard Test Method for Density, Absorption, and Voids in Hardened Concrete. *ASTM C 642*, ASTM Philadelphia.
20. TS EN 1015-11. (2002). Methods of test for mortar for masonry. Determination of flexural and compressive strength of hardened mortar. *TS EN 1015-11*, TSE Ankara, (in Turkish).
21. Mehta, P. K. (1981). Studies on blended portland cements containing Santorin Earth. *Cement and Concrete Research*, Vol. 4, pp. 507–518.
22. Kockal, N. U. & Ozturan, T. (2011). Durability of lightweight concretes with lightweight fly ash aggregates. *Construction and Building Materials*, Vol. 25, pp. 1430–1438.
23. Ganjian, E. & Pouya, H. S. (2009). The effect of Persian Gulf tidal zone exposure on durability of mixes containing silica fume and blast furnace slag. *Construction and Building Materials*, Vol. 23, pp. 644–652.
24. Jain, N. (2012). Effect of nonpozzolanic and pozzolanic mineral admixtures on the hydration behavior of ordinary Portland cement. *Construction and Building Materials*, Vol. 27, pp. 39–44.
25. Li, H., Xiao, H. G. & Ou, J. P. (2004). A study on mechanical and pressure-sensitive properties of cement mortar with nano phase materials. *Cement and Concrete Research*, Vol. 34, pp. 435–438.
26. Sadrmmomtazi, A. & Fasihi, A. (2010). Influence of polypropylene fibers on the performance of nano-SiO₂-incorporated mortar. *Iranian Journal of Science & Technology, Transaction B: Engineering*, Vol. 34, pp. 385–395.
27. Alp, I., Deveci, H., Sungun, Y. H., Yilmaz, A. O., Kesimal, A. & Yilmaz, E. (2009). Pozzolanic characteristics of a natural raw material for use in blended cements. *Iranian Journal of Science & Technology, Transaction B: Engineering*, Vol. 33, pp. 291–300.
28. O'Farrell, M., Sabir, B. B. & Wild, S. (2006). Strength and chemical resistance of mortars containing brick manufacturing clays subjected to different treatments. *Cement and Concrete Composites*, Vol. 28, pp. 790–799.
29. Changling, H., Osbaeck, B. & Makovsky, E. (1995). Pozzolanic reactions of six principal clay minerals: Activation, reactivity assessments and technological effects. *Cement and Concrete Research*, Vol. 25, pp. 1691–1702.
30. Xuan, D. X. & Shui, Z. H. (2011). Rehydration activity of hydrated cement paste exposed to high temperature. *Fire and Materials*, Vol. 35, pp. 481–490.